ORGANIC LETTERS

2011
Vol. 13, No. 24
6528–6531

Charge Transport Anisotropy in *n*-Type Disk-Shaped Triphenylene-Tris(aroyleneimidazole)s

Yue Zhang,[†] David Hanifi,[†] Steven Alvarez,[‡] Francisco Antonio,[†] Andrew Pun,[†] Liana M. Klivansky,[†] Alexander Hexemer,[‡] Biwu Ma,*[,†] and Yi Liu*[,†]

The Molecular Foundry and Advanced Light Source, Lawrence Berkeley National Laboratory, One Cyclotron Road, Berkeley, California 94720, United States

yliu@lbl.gov; bwma@lbl.gov

Received October 19, 2011

ABSTRACT

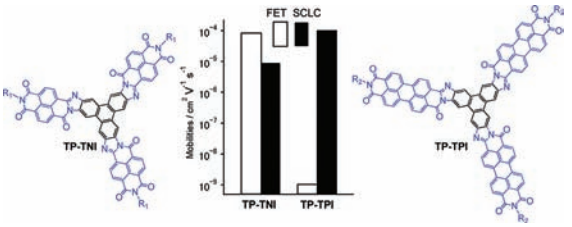

Two novel *n*-type disk-shaped molecules containing a triphenylene core and three fused naphthaleneimide imidazole or peryleneimide imidazole "arms" are synthesized and characterized. The *n*-type charge carrier mobilities of these molecules are evaluated by both field effect transistors and space-charge limited-current measurements, which exhibit drastically different mobility anisotropy. A strong correlation between film morphology and the charge transport behavior is established by X-ray scattering and atomic force microscopic analyses.

Organic semiconductors with controllable molecular packing and long-range ordering are of great interest for the development of high-performance electronic devices, such as organic field-effect transistors (OFET)[1] and organic photovoltaics (OPVs).[2] While charge carrier mobility is the key parameter in describing organic semiconductors, the devices are also dependent on the directionality of charge transport and the associated anisotropy.[3] Charge transport in the lateral direction favors high FET performance, while the vertical charge transport is desirable for diode-type devices such as OPVs.[4] Disk-shaped molecules containing polycyclic aromatic cores have a strong propensity for stacking into 1D columns as the preferred charge transporting pathway,[4,5] and thus emerge as a promising class of organic semiconductors with controllable transport anisotropy.[3b] In terms of charge carrier types, both *p*-type (hole conducting) and *n*-type (electron conducting) semiconductors are required for the fabrication of complementary logic circuits[6] or for use as active materials in OPVs.[2] A number of *p*-type disk-shaped molecules with mobilities comparable to or even

[†] The Molecular Foundry.
[‡] Advanced Light Source.

(1) (a) Murphy, A. R.; Fréchet, J. M. J. *Chem. Rev.* **2007**, *107*, 1066–1096. (b) Muccini, M. *Nat. Mater.* **2006**, *5*, 605–613. (c) Katz, H. E.; Bao, Z. N.; Gilat, S. L. *Acc. Chem. Res.* **2001**, *34*, 359–369.

(2) (a) (c) Wallace, W.; Wong, H.; Singh, T. B.; Vak, D.; Pisula, W.; Yan, C.; Feng, X.; Williams, E. L.; Leok, K. L.; Mao, Q.; Jones, D. J.; Ma, C.-Q.; Müllen, K.; Bäuerle, P.; Holmes, A. B. *Adv. Funct. Mater.* 2010, *20*, 927-938. (b) Hains, A. W.; Liang, Z.; Woodhouse, M. A.; Gregg, B. A. *Chem. Rev.* **2010**, *110*, 6689–6735. (c) Brédas, J.-L.; Norton, J. E.; Cornil, J.; Coropceanu, V. *Acc. Chem. Res.* **2009**, *42*, 1691–1699. (d) Peet, J.; Heeger, A. J.; Bazan, G. C. *Acc. Chem. Res.* **2009**, *42*, 1700–1708. (e) Zhang, Y.; Tajima, K.; Hirota, K.; Hashimoto, K. *J. Am. Chem. Soc.* **2008**, *130*, 7812–7813. (f) Günes, S.; Neugebauer, H.; Sariciftci, N. S. *Chem. Rev.* **2007**, *107*, 1324–1338. (g) Schmidt-Mende, L.; Fechtenkotter, A.; Müllen, K.; Moons, E.; Friend, R. H.; Mackenzie, J. D. *Science* **2001**, *293*, 1119–1122.

(3) (a) Huang, Y. F.; Chang, C. W.; Smilgies, D.-M.; Jeng, U. S.; Inigo, A. R.; White, J. D.; Li, K. C.; Lim, T. S.; Li, T. D.; Chen, H. Y.; Chen, S. A.; Chen, W. C.; Fann, W. S. *Adv. Mater.* **2009**, *21*, 2988–2992. (b) Shklyarevskiy, I. O.; Johkheijm, P.; Stutzmann, N.; Wasserberg, D.; Wondergem, H. J.; Christianen, P. C. M.; Shcenning, A. P. H. J.; de Leeuw, D. M.; Tomović, Ž.; Wu, J.; Müllen, K.; Man, J. C. *J. Am. Chem. Soc.* **2005**, *127*, 16233–16237. (c) Nishizawa, T.; Lim, H. K.; Tajima, K.; Hashimoto, K. *J. Am. Chem. Soc.* **2009**, *131*, 2464–2465.

(4) Wu, J.-S.; Pisula, W.; Müllen, K. *Chem. Rev.* **2007**, *107*, 718–747.

(5) (a) Laschat, S.; Baro, A.; Steinke, N.; Giesselmann, F.; Hagele, C.; Scalia, G.; Judele, R.; Kapatsina, E.; Sauer, S.; Schreivogel, A.; Tosoni, M. *Angew. Chem., Int. Ed.* **2007**, *46*, 4832–4887. (b) Sergeyev, S.; Pisula, W.; Geerts, Y. H. *Chem. Soc. Rev.* **2007**, *36*, 1902–1929. (c) Kato, T.; Yasuda, T.; Kamikawa, Y.; Yoshio, M. *Chem. Commun.* **2009**, 729–739.

(6) Klauk, H.; Zschieschang, U.; Pflaum, J.; Halik, M. *Nature* **2007**, *445*, 745–748.

10.1021/ol202814y
Published on Web 11/14/2011

surpassing that of amorphous silicon have been developed over the past decades, including triphenylenes,[7] phthalocyanines,[8] porphyrins,[9] hexabenzocoronene,[10] and truxenes.[11] In contrast, *n*-type disk-shaped molecular systems are still much underdeveloped.[12] Even more so, there lacks a detailed study of their electronic properties in the context of thin film devices.

n-Type naphthalenetetracarboxylic diimide (NDI) and perylenetetracarboxylic diimide (PDI)-based materials have become increasingly attractive due to their high charge-carrier mobilities, superior light absorption in the wavelength range of visible light, and high thermal, chemical, and photostability.[13] Incorporating these electron-deficient units into c_3-symmetric disk-shaped molecular skeletons poses as an appealing approach toward achieving good optical, electronic, and self-assembly properties.[12e] Herein, we report the investigation of a series of novel *n*-type disk-shaped molecules that contain a triphenylene core fused with three naphthaleneimide imidazole or peryleneimide imidazole "arms" (Scheme 1). As a result of extended conjugation, the fusion has led to enhanced optical properties along with well-aligned frontier orbital energies. Moreover, charge carrier mobilities of these compounds, measured both in the context of field effect transistors and by the space-charge limited-current (SCLC) model, show drastically different directional anisotropy. As revealed by X-ray scattering and atomic force microscopic (AFM) analyses, a strong correlation between the film morphology and the charge transport behavior has been established.

Scheme 1. Synthetic Scheme and Molecular Structures of **TP-TNI**, **TP-TPI**, **NI**, and **PI**[a]

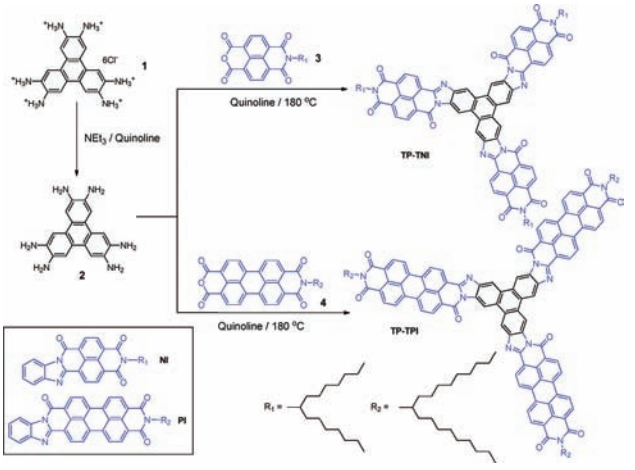

[a] **TP-TNI** and **TP-TPI** are obtained as a mixture of symmetric and asymmetric isomers, with only the structures of symmetric ones shown.

Scheme 1 shows the synthesis of the naphthaleneimide-based trimer **TP-TNI**, the peryleneimide-based trimer **TP-TPI**, and their respective single "arm" counterparts, i.e. naphthaleneimide imidazole (**NI**) and peryleneimide imidazole (**PI**). The trimeric **TP-TNI** and **TP-TPI** are obtained as a statistical mixture of *cis*- (symmetric) and *trans*- (asymmetric) isomers from the condensation reaction between hexaaminotriphenylene and the corresponding anhydrides. Branched swallow-tail alkyl chains are employed as the imide substituent to endow good solubility in common organic solvents. Both **TP-TNI** and **TP-TPI** give very broad NMR spectra across a wide range of temperatures. Nevertheless, their identities are fully supported by mass spectrometry and elementary analyses. The trimers are thermally stable above 400 °C as revealed by thermogravimetric analysis (TGA). No thermal transitions could be observed in differential scanning calorimetry (DSC) in a wide temperature range from 20 to 350 °C at various scanning rates (10 and 2 °C min^{-1}) (Figures S1–S2, Supporting Information, SI).

The optical properties of these compounds are investigated in both solution and thin film. The UV–vis spectra of **TP-TNI** and **TP-TPI** in $CHCl_3$ solution reveal (Figure 1a) broad absorption in the visible region, with maxima at 502 nm (ε = 25 600 M^{-1} cm^{-1}) and 624 nm (ε = 49 200 M^{-1} cm^{-1}), respectively. The absorption spectrum of **TP-TNI** is significantly red-shifted as compared to those of monomeric **NI** as a result of more extensive

(7) (a) Kumar, S. *Liq. Cryst.* **2004**, *31*, 1037–1059. (b) Sarhan, A. A. O.; Bolm, C. *Chem. Soc. Rev.* **2009**, *38*, 2730–2744.

(8) (a) Chu, C.-W.; Shrotriya, V.; Li, G.; Yang, Y. *Appl. Phys. Lett.* **2006**, *88*, 1535041–3. (b) Fischer, M. K. R.; López-Duarte, I.; Wienk, M. M.; Martínez-Díaz, M. V.; Janssen, R. A. J.; Bäuerle, P.; Torres, T. *J. Am. Chem. Soc.* **2009**, *131*, 8669–8676. (c) de la Escosura, A.; Martínez-Díaz, M. V.; Torres, T.; Grubbs, R. H.; Guldi, D. M.; Neugebauer, H.; Winder, C.; Drees, M.; Sariciftci, N. S. *Chem.—Asian J.* **2006**, *1*–*2*, 148–154.

(9) (a) Sun, Q.; Dai, L.; Zhou, X.; Li, L.; Li, Q. *Appl. Phy. Lett.* **2007**, *91*, 253505/1–253505/3. (b) Sakurai, T.; Tashiro, K.; Honsho, Y.; Saeki, A.; Seki, S.; Osuka, A.; Muranaka, A.; Uchiyama, M.; Kim, J.; Ha, S.; Kato, K.; Takata, M.; Aida, T. *J. Am. Chem. Soc.* **2011**, *133*, 6537–6540.

(10) (a) Shklyarevskiy, I. O.; Jonkheijm, P.; Stutzmann, N.; Wasserberg, D.; Wondergem, H. J.; Christianen, P. C. M.; Schenning, A. P. H. J.; de Leeuw, D. M.; Tomović, Ž.; Wu, J. S.; Müllen, K.; Maan, J. C. *J. Am. Chem. Soc.* **2005**, *127*, 16233–16237. (b) Xiao, S.; Tang, J.; Beetz, T.; Guo, X.; Tremblay, N.; Siegrist, T.; Zhu, Y.; Steigerwald, M.; Nuckolls, C. *J. Am. Chem. Soc.* **2006**, *128*, 10700–10701. (c) Plunkett, K. N.; Godula, K.; Nuckolls, C.; Tremblay, N.; Whalley, A. C.; Xiao, S. X. *Org. Lett.* **2009**, *11*, 2225–2228.

(11) (a) Luo, J.; Zhou, Y.; Niu, Z.-Q.; Zhou, Q.-F.; Ma, Y.; Pei, J. *J. Am. Chem. Soc.* **2007**, *129*, 11314–11315. (b) Zhao, B.; Liu, B.; Png, R. Q.; Zhang, K.; Lim, K. A.; Luo, J.; Shao, J.; Ho, P. K. H.; Chi, C.; Wu, J.-S. *Chem. Mater.* **2010**, *22*, 435–449.

(12) (a) McMenimen, K. A.; Hamilton, D. G. *J. Am. Chem. Soc.* **2001**, *123*, 6453–6454. (b) Pieterse, K.; van Hal, P. A.; Kleppinger, R.; Vekemans, J. A. J. M.; Janssen, R. A. J.; Meijer, E. W. *Chem. Mater.* **2001**, *13*, 2675–2679. (c) Kestemont, G.; de Halleux, V.; Lehmann, M.; Ivanov, D. A.; Watson, M.; Geerts, Y. H. *Chem. Commun.* **2001**, 2074–2075. (d) Yin, J; Qu, H.; Zhang, K.; Luo, J.; Zhang, X.; Chi, C.; Wu, J.-S. *Org. Lett.* **2009**, *11*, 3028–3031. (e) Hanifi, D.; Cao, D.; Klivansky, L. M.; Liu, Y. *Chem. Commun.* **2010**, *47*, 3454–3456. (f) Ishi-i, T.; Yaguma, K.; Kuwahara, R.; Taguri, Y.; Mataka, S. *Org. Lett.* **2006**, *8*, 585–588. (g) Ong, C. W.; Liao, S.-C.; Chang, T. H.; Hsu, H.-F. *J. Org. Chem.* **2004**, *69*, 3181–3185. (h) Sakurai, T.; Shi, K. Y.; Sato, H.; Tashiro, K.; Osuka, A.; Saeki, A.; Seki, S.; Tagawa, S.; Sasaki, S.; Masunaga, H.; Osaka, K.; Takata, M.; Aida, T. *J. Am. Chem. Soc.* **2008**, *130*, 13812–13813. (i) Loo, Y.-L.; Hiszpanski, A. M.; Kim, B. J.; Wei, S. J.; Chiu, C. Y.; Steigerwald, M. L.; Nuckolls, C. *Org. Lett.* **2010**, *12*, 4840–4843.

(13) (a) Jones, B. A.; Facchetti, A.; Wasielewski, M. R.; Marks, T. J. *J. Am. Chem. Soc.* **2007**, *129*, 15259–15278. (b) Jones, B. A.; Facchetti, A.; Marks, T. J.; Wasielewski, M. R. *Chem. Mater.* **2007**, *19*, 2703–2705. (c) See, K. C.; Landis, C.; Sarjeant, A.; Katz, H. E. *Chem. Mater.* **2008**, *20*, 3609–3616. (d) Che, Y.; Datar, A.; Balakrishnan, K.; Zang, L. *J. Am. Chem. Soc.* **2007**, *129*, 7234–7235. (e) An, Z.; Yu, J.; Jones, S. C.; Barlow, S.; Yoo, S.; Domercq, B.; Prins, P.; Siebbeles, L. D. A.; Kippelen, B.; Marder, S. R. *Adv. Mater.* **2005**, *17*, 2580–2583.

electron delocalization in the trimeric polycyclic aromatic cores. The fine absorption bands in the **TP-TPI** spectrum show a hypsochromic shift when compared to the **PI** monomer, together with an additional broad shoulder at longer wavelength. The hypsochromic shift suggests H-aggregation in the solution, while the broad featureless band might originate from intramolecular charge transfer. The UV−vis spectra of spuncast thin films of **TP-TNI** and **TP-TPI** show a bathochromic red shift (ca. 30 nm) when compared to the corresponding solution spectra, ascribable to enhanced $\pi-\pi$ intermolecular interactions in thin films. From the onset of their long wavelength absorption spectra (670 nm for **TP-TNI** and 770 nm for **TP-TPI**), the respective optical band gaps are estimated to be 1.9 and 1.7 eV. From the cyclic voltammetry (CV) measurements (Figure S3, SI), the lowest unoccupied molecular orbital (LUMO) energy levels of **TP-TNI** and **TP-TPI** are measured to be −3.7 eV (Figure 1b). The low-lying LUMO energies of **TP-TNI** and **TP-TPI** suggest their potential as *n*-type semiconductor materials. The highest occupied molecular orbital (HOMO) energy levels are calculated to be −5.7 and −5.3 eV for **TP-TNI** and **TP-TPI**, respectively, from the difference between the LUMO and optical band gap.

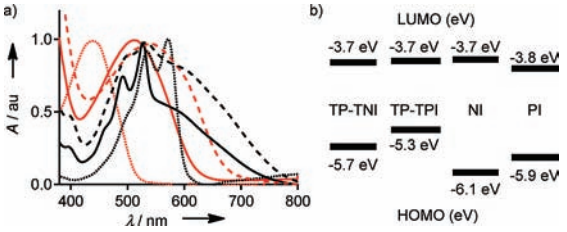

Figure 1. (a) UV−vis spectra of **NI** (red dotted line), **PI** (black dotted line), **TP-TNI** (red solid line) and **TP-TPI** (black solid line) in $CHCl_3$, and thin films of **TP-TNI** (red dashed line) and **TP-TPI** (black dashed line). (b) Relative positions of their frontier orbital energy levels.

Lateral charge transporting properties of these materials are evaluated in FETs (Figure 2), using the bottom gate/top contact OFET configuration with octyldecyltrichlorosilane (OTS)-modified SiO_2 as the dielectric layer.[14] Gold (Au) is used as the source/drain electrodes unless mentioned otherwise, and the scratched *n*-doped Si works as the gate electrode. All samples are prepared by spin coating organic solutions of active materials on OTS-SiO_2, resulting in thin films with a thickness of ∼20−30 nm. The highest lateral electron mobility ($\mu_{//}$) of **TP-TNI** is 1.3×10^{-4} cm^2 V^{-1} s^{-1} (Table S1, SI), which is among the highest FET electron mobilities for solution processed disk-shaped *n*-type molecules.[12,15] The on/off ratio is on the order of 10^3-10^4. In contrast, the mobility of the corresponding monomer **NI** is more than 4 orders of magnitude smaller. Devices with Al as source/drain electrodes also showed a similar tendency. For perylene-based derivatives, the highest $\mu_{//}$ of the monomeric **PI** is 1.4×10^{-5} cm^2 V^{-1} s^{-1}. Surprisingly, the carrier mobility of **TP-TPI**-based transistors is very low (∼10^{-9} cm^2 V^{-1} s^{-1}) regardless of the nature of the evaporated top electrodes (Au, Al, or Ca/Al).

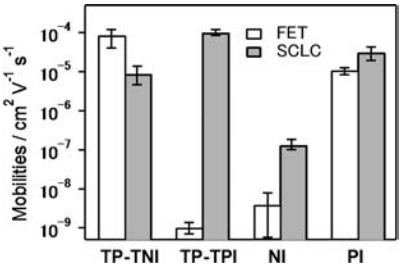

Figure 2. Comparison of FET (empty bar) and SCLC (gray bar) electron mobilities of **TP-TNI**, **TP-TPI**, **NI**, and **PI**.

Vertical charge carrier mobilities ($\mu_\perp$) are measured using the SCLC model for the spuncast thin films (50−120 nm) sandwiched between indium tin oxide (ITO) and Al electrodes (Table S2, SI). In sharp contrast to **TP-TPI**'s poor lateral charge transporting characters, the $\mu_\perp$ is measured to be 1.3×10^{-4} cm^2 V^{-1} s^{-1}, corresponding to a mobility anisotropy ($\mu_\perp/\mu_{//}$) of more than 10^5 (Figure 2). The charge transport in **TP-TNI** is more balanced. The SCLC $\mu_\perp$ is measured to be 1.6×10^{-5} cm^2 V^{-1} s^{-1}, resulting in the value of $\mu_\perp/\mu_{//}$ several orders smaller than that of **TP-TPI**. For the monomeric **NI** and **PI**, the $\mu_\perp/\mu_{//}$ values are around 10^1-10^2 and 10^0-10^1, also several orders smaller.

To gain a better understanding of the dramatic difference in transport anisotropy of these disk-shaped molecules, synchrotron grazing incidence wide-angle X-ray scattering (GIWAXS) and AFM studies are carried out to investigate the thin film morphologies. The GIWAXS pattern of the **TP-TNI** thin film corresponds (Figure 3a) to a typical hexagonal columnar packing, with the columns laying parallel to the substrate. The *Q*-plot shows (red curve, Figure 3b) a *d*-spacing of 3.4 Å in the horizontal line cut, indicative of $\pi-\pi$ interactions between the disk-shaped molecules in the lateral direction.[16] In contrast, there is no vertical $\pi-\pi$ stacking as suggested by the absence of scattering peaks in the vertical profile (black curve, Figure 3b). A 3.4 nm intercolumnar distance can be derived from the *d*-spacing of 3.0 nm, which correlates to the footprint of **TP-TNI**. The *d*-spacing of 2.5 nm on the

(14) Maliakal, A. In *Organic Field-Effect Transistors*, Vol. 128; Bao, Z., Locklin, J., Eds.; CRC Press: Boca Raton, FL, 2007.

(15) (a) Zhang, Y.-D.; Jespersen, K. G.; Kempe, M.; Kornfield, J. A.; Barlow, S.; Kippelen, B.; Marder, S. R. *Langmuir* **2003**, *19*, 6534–6536. (b) Iino, H.; Takayashiki, Y.; Hanna, J.-I.; Bushby, R. J. *Jpn. J. Appl. Phys.* **2005**, *44*, L1310–1312. (c) Iino, H.; Takayashiki, Y.; Hanna, J.-I. *Appl. Phys. Lett.* **2005**, *87*, 1921051–3.

(16) Allen, M. T.; Diele, S.; Harris, K. D. M.; Hegmann, T.; Kariuki, B. M.; Lose, D.; Preece, J. A.; Tschierske, C. *J. Mater. Chem.* **2001**, *11*, 302–311.

vertical direction is tentatively assigned to the coexistence of lamellar structures. Based on the GIWAXS data, an "edge-on" packing model is postulated with the "Y"-shaped disks arranged into face-to-face π-stacked columns (Figure 3d, left). The parallel aligned hexagonal columns in **TP-TNI** thin film facilitates the charge-carrier transport in an FET configuration. The good lateral mobilities are also supported by AFM studies, which illustrate the formation of a continuous film with a smooth surface and small domain sizes (Figure S7a, SI).

On the other hand, the GIWAXS of **TP-TPI** indicates an amorphous film despite some characteristic scattering peaks (Figure S6, SI). The horizontal line cut of the *Q*-plot shows a *d*-spacing of 4.4 Å that is ascribable to the center-to-center distance of adjacent slip-packed aromatic planes, which translates to a face-to-face interplanar distance of ~3.5 Å (Figure 3c).[17] The small peak on the vertical line cut reveals a *d*-spacing of 2.1 nm. It can be assigned to the (002) scattering that correlates to the 4.2 nm molecular size of **TP-TPI**. Although **TP-TPI** molecules appear to have some orientational order in the lateral direction, overall the film is quite amorphous and the poor molecular ordering in the thin film introduces structural defects that work as trapping sites for lateral charge transport. In addition, AFM images of **TP-TPI** film show (Figure S7c, SI) much rougher film morphology than that of **TP-TNI**. The presence of large discontinuous domains leads to boundaries that significantly increase the lateral electron transport barrier.[18] Despite the lack of long-range ordering, the "Y" shaped **TP-TPI** molecules are well positioned to form an intercalated π-stacking network across the film through partial π-surface overlap of their extended conjugated "arms" (Figure 3d, right). Such π-stacking results in a vertically interconnected, continuous hopping pathway that is responsible for good SCLC mobilities.

In summary, novel *n*-type disk-shaped molecules **TP-TNI** and **TP-TPI** have been constructed from a triphenylene core and three fused naphthaleneimide and peryleneimide arms. As a result of the fusion, **TP-TNI** exhibits 4−5 orders of magnitude higher lateral electron mobility in thin film transistors than the corresponding monomeric **NI**. Such a trend is however reversed in the peryleneimide-based system. SCLC measurements indicate remarkable charge transport anisotropy in **TP-TPI** while, in the case of **TP-TNI**, the charge transport is more isotropic. Correlated with X-ray scattering and AFM studies, the observed transport anisotropy for **TP-TPI** suggests that there lacks a connected pathway on the lateral direction while the molecules are more interconnected along the vertical direction due to slipped π-stacking and large domains.

(17) (a) Che, Y.; Yang, X.; Liu, G.; Yu, C.; Ji, H.; Zuo, J.; Zhao, J.; Zang, L. *J. Am. Chem. Soc.* **2010**, *132*, 5743–5750. (b) Koshkakaryan, G.; Jiang, P.; Cao, D.; Klivansky, L. M.; Altoe, V.; Zhang, Y.; Ma, B.; Salmeron, M.; Aloni, S.; Liu, Y. *Chem. Commun.* **2010**, *46*, 8579–8581.

(18) Kelley, T. W.; Frisbie, C. D. *J. Phys. Chem. B* **2001**, *105*, 4538–4540.

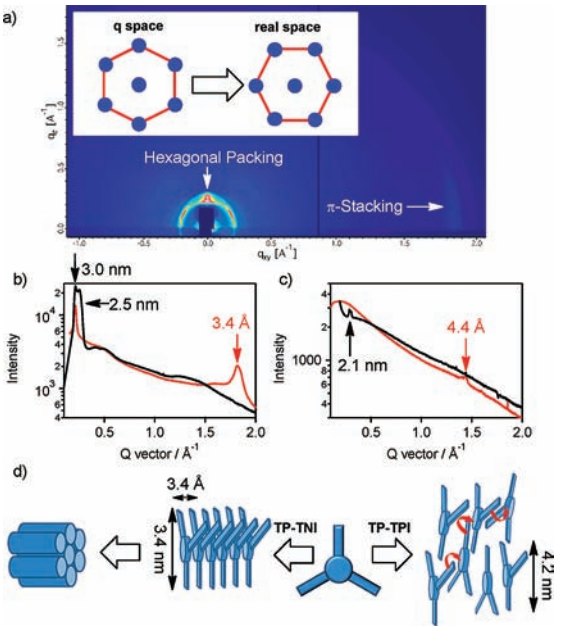

Figure 3. (a) GIWAXS pattern of **TP-TNI**. The inset shows the correlation between scattering pattern in *q*-space and the real space molecular ordering in a hexagonal lattice. (b and c) Respective *q*-plots of **TP-TNI** and **TP-TPI** thin films. Red and black solid lines show the horizontal and vertical line cuts. (d) Proposed molecular packings in **TP-TNI** (left) and **TP-TPI** (right) in thin films. The red arrow indicates the possible electron hopping pathway within the intercalated π-stacking network across the **TP-TPI** film.

On the other hand, the **TP-TNI** molecules are arranged into more ordered hexagonal packing with edge-on orientation in thin films. The difference in molecular ordering is probably a result of a larger void space and higher reorganization cost due to the increased molecular size of **TP-TPI**. Nevertheless, the structures of disk-shaped trimeric molecules can be readily tuned for further improvement of molecular orientation and long-range ordering in thin films, and thus, hold great promise as a new class of high performance *n*-type organic semiconductors.

Acknowledgment. This work was performed at the Molecular Foundry, and the X-ray scattering experiment was performed at the Advanced Light Source, Lawrence Berkeley National Laboratory, both supported by the Office of Science, Office of Basic Energy Sciences, Scientific User Facilities Division, of the U.S. Department of Energy under Contract No. DE-AC02-05CH11231.

Supporting Information Available. Synthetic details of all the new compounds. Device fabrication and characterization details and AFM studies. This material is available free of charge via the Internet at http://pubs.acs.org.